Journal of Steroid Biochemistry & Molecular Biology 121 (2010) 84–87

Contents lists available at ScienceDirect

Journal of Steroid Biochemistry and Molecular Biology

journal homepage: www.elsevier.com/locate/jsbmb

Crystal structure of hereditary vitamin D-resistant rickets—Associated mutant H305Q of vitamin D nuclear receptor bound to its natural ligand☆

Natacha Rochel*, Shinji Hourai, Dino Moras**

IGBMC (Institut de Génétique et de Biologie Moléculaire et Cellulaire), Département de Biologie et de Génomique Structurales, Centre National de la Recherche Scientifique, Institut National de la Santé de la Recherche Médicale, Université de Strasbourg, 1 rue Laurent Fries, Illkirch, France

ARTICLE INFO

Article history:
Received 17 March 2010
Accepted 9 April 2010

Keywords:
VDR mutant rickets
Calcitriol
Crystal structure

ABSTRACT

In the nuclear receptor of vitamin D (VDR) histidine 305 participates to the anchoring of the ligand. The VDR H305Q mutation was identified in a patient who exhibited the hereditary vitamin D-resistant rickets (HVDRR). We report the crystal structure of human VDR H305Q-ligand binding domain bound to 1α,25(OH)$_2$D$_3$ solved at 1.8 Å resolution. The protein adopts the active conformation of the wild-type liganded VDR. A local conformational flexibility at the mutation site weakens the hydrogen bond between the 25-OH with Gln305, thus explaining the lower affinity of the mutant proteins for calcitriol. The structure provides the basis for a rational approach to the design of more potent ligands for the treatment of HVDRR.

1. Introduction

The vitamin D receptor mediates genomic actions upon binding of 1α,25-dihydroxyvitamin D3, the active form of the seco-steroid hormone vitamin D [1–4]. 1α,25(OH)$_2$D$_3$ (Fig. 1) is an important regulator of bone development and metabolism and calcium homeostasis. It also plays an important role in the regulation of cell growth and differentiation. Mutations in the VDR gene cause the rare genetic disorder hereditary vitamin D-resistant rickets (HVDRR) or vitamin D-dependent type II rickets (VDRRII). Patients with this disease display rickets, hypocalcemia and secondary hyperparathyroidism (review in Refs. [5–7]). Among the identified mutations are missence mutations, nonsense mutations, splicing and partial gene deletions that affect DNA binding or ligand dependent transactivation functions of VDR [8–10]. Some of the mutations were found in the ligand binding domain (LBD) of the VDR receptor and have been shown to affect ligand binding, RXR heterodimerization and co-activator interaction and result in partial or total response to the hormone [8,9,11–14]. One of these mutations, H305Q identified in a HVDRR patient, is associated with a 10-fold decrease in 1α,25(OH)$_2$D$_3$-dependent transactivation and an eightfold lower affinity for calcitriol than the normal VDR [11].

We have previously reported crystal structures of the VDR ligand binding domain (LBD) in complexes with 1α,25(OH)$_2$D$_3$ or synthetic agonists, and have shown that all compounds are anchored by the same residues in the ligand binding pocket (LBP) with the hydroxyls of the A-ring and of the side chain located in identical position and forming the same hydrogen bonds [15–17]. In order to understand the mechanism underlying the dysfunction of the VDR H305Q mutant, we have solved the crystal structure of its complex with 1α,25(OH)$_2$D$_3$. This structural data are of therapeutic interest and will help to design specific ligands for this VDR mutant.

2. Materials and methods

2.1. Purification and crystallization

The LBD of the human VDR His305Gln mutant (residues 118–427 Δ165–215) was cloned in pET28b expression vector to obtain an N-terminal hexahistidine-tagged fusion protein and was overproduced in *E. coli* BL21 (DE3) strain. Cells were grown in LB medium and subsequently induced for 6 h at 20 °C with 1 mM isopropyl thio-β-D-galactoside. Purification and crystallization were similar to hVDR LBD complex with 1α,25(OH)$_2$D$_3$ [15]. The purification included a metal affinity chromatography step on a cobalt-chelating resin. After tag removal by thrombin digestion, the protein was further purified by gel filtration. The final protein buffer was 10 mM Tris, pH 7.5, 100 mM NaCl, and 5 mM DTT (dithiothreitol). The protein was then concentrated to 10 mg/mL and incubated in the presence of a 5-fold excess of ligand. The later was purchased from SIGMA, dissolved in ethanol at a concentration of 10^{-2} M and stored at −20 °C. The purity and homogeneity

Abbreviations: NR, nuclear receptor; VDR, vitamin D NR; LBD, ligand binding domain; LBP, ligand binding pocket.

☆ Special issue selected article from the 14th vitamin D workshop held at Brugge, Belgium on October 4–8 2009.

* Corresponding author. Tel.: +33 388 655 781; fax: +33 388 653 276.
** Corresponding author. Tel.: +33 388 653 220; fax: +33 388 653 276.
E-mail addresses: rochel@igbmc.fr (N. Rochel), moras@igbmc.fr (D. Moras).

0960-0760/$ – see front matter © 2010 Elsevier Ltd. All rights reserved.
doi:10.1016/j.jsbmb.2010.04.008

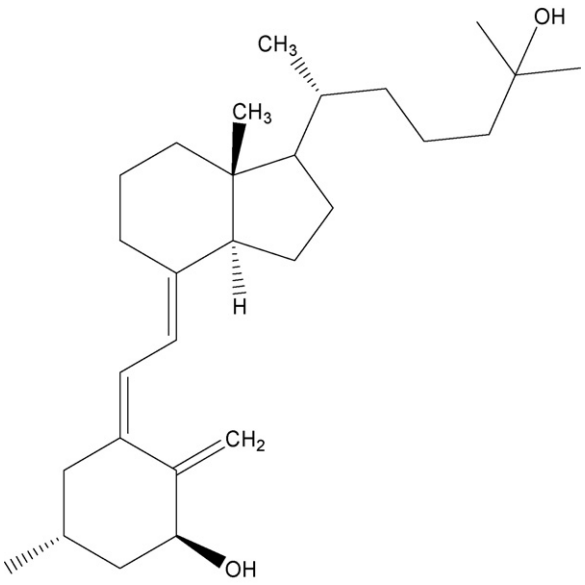

Fig. 1. Chemical structure of 1α,25-dihydroxyvitamin D_3.

Table 1
Data collection and refinement statistics.

	VDR H305Q/1α,25(OH)$_2$D$_3$
Data processing	
Resolution (Å)	20.0–1.8
Crystal space group	$P2_12_12_1$
Cell parameters (Å)	a = 44.40, b = 51.67, c = 131.89
Unique reflections	28029
R_{sym} (%)[a]	8.3 (27.5)
Completeness (%)	96.9 (97.8)
Refinement	
Number of protein atoms	2011
Number of ligand atoms	30
Number of water molecules	164
R.m.s.d. bond length (Å)[b]	0.004
R.m.s.d. bond angles (°)[b]	1.05
R_{cryst} (%)[c]	21.1
R_{free} (%)[c]	24.1

Values in parentheses correspond to the highest resolution shell.
[a] R_{sym} $(I) = \Sigma_{hkl}\Sigma_i|I_{hkl,i} - \langle I_{hkl}\rangle|/\Sigma_{hkl}\Sigma_i|I_{hkl,i}|$ with $\langle I_{hkl}\rangle$ the mean intensity of the multiple $I_{hkl,i}$ observations for symmetry-related reflections.
[b] Root-mean-squared deviations (R.m.s.d.) are given from ideal values.
[c] $R_{cryst} = \Sigma_{hkl}|F_{obs} - F_{calc}|/\Sigma_{hkl}|F_{obs}|$, where F_{obs} and F_{calc} are the observed and calculated structure amplitudes, respectively. R_{free} is the same as R_{cryst}, but calculated on the 10% of data excluded from refinement.

of the protein were assessed by SDS-PAGE and Native-PAGE. Crystals were obtained at 4 °C by vapour-diffusion in hanging drops. Crystals of wild-type VDR LBD-1α,25(OH)$_2$D$_3$ complex were used for micro-seeding. The seeds from serial dilutions were introduced into freshly made drops. The reservoir solutions contained 0.1 M Mes and 1.4 M ammonium sulphate at pH 6.0.

2.2. X-ray data collection and structure determination

Crystals were mounted in fiber loops and flash cooled in liquid ethane at liquid nitrogen temperature after cryoprotection with a solution containing the reservoir solution plus 30% glycerol and 5% PEG400. Data collection from a single frozen crystal was performed at 100 K at the beamline BM30 of ESRF (Grenoble, France). Diffraction data were integrated and scaled using the HKL2000 program package [18]. A rigid body refinement was performed using the structure of the hVDR LBD/1α,25(OH)$_2$D$_3$ complex as a starting model. Refinement involved iterative cycles of manual building and refinement calculations. The programs CNS [19] and O [20] were used throughout structure determination and refinement. The ligand molecule was included only at the last stage of the refinement. Anisotropic scaling and bulk solvent correction were used. Individual atomic *B* factors were refined isotropically. Solvent molecules were then placed according to unassigned peaks in the difference Fourier map. All data were included in the refinement (no δ-cutoffs). All refined models showed unambiguous chirality for the ligands and no Ramachandran plot outliers according to PROCHECK. The final model lacks the first two N-terminal residues and the last four C-terminal residues, because of no electron density for these regions. For the structure comparison, Cα traces of the models were superimposed using the lsq commands of O and default parameters. The figures were generated with Pymol (http://www.pymol.org/).

3. Results and discussion

3.1. Overall structures of the hVDR H305Q LBD bound to 1α,25(OH)$_2$D$_3$

To obtain crystals of the VDR H305Q-ligand complex, we used a human VDR LBD construct that lacks 50 residues in the loop connecting helices H1 and H3. The same construct was used to solve the structures of hVDR LBD in complex with 1α,25(OH)$_2$D$_3$ and several analogues since its biological properties, such as ligand binding and transactivation in distinct cell lines, are the same as those of the wild-type protein [15–17,21]. Crystals were obtained in similar conditions and are isomorphous. The crystal structure of hVDR H305Q LBD bound to 1α,25(OH)$_2$D$_3$ was determined at a resolution of 1.8 Å (Table 1).

The VDR H305Q-1α,25(OH)$_2$D$_3$ complex adopts the canonical conformation of all previously reported agonist-bound nuclear receptor LBD with 12 α-helices organized in a 3-layered sandwich. The position and conformation of the activation helix-12 is strictly maintained. The atomic models, when compared with wild VDR-1α,25(OH)$_2$D$_3$ complex, show root-mean-square-deviation (r.m.s.d.) on Cα atoms of 0.37 Å.

3.2. Ligand binding

The omit map from the refined atomic model of VDR LBD H305Q was used to fit the ligand to the electron density as shown in Fig. 2. The conformation of the calcitriol is similar to that observed in the wild-type VDR crystal structure with similar conformations of the A-, seco-B-, C- and D-rings (Fig. 3). The previously reported crystal structures of hVDR LBD in complex with 1α,25(OH)$_2$D$_3$ and several synthetic ligands revealed the presence of tightly bound water molecules forming a channel near the C2 position of the ligand, which may play important roles in protein stability [15]. This water channel is also conserved in the present mutant complex.

The interactions between the receptor and the ligand involve both hydrophobic and electrostatic contacts. The 1-OH and 3-OH hydroxyl groups make the same hydrogen bonds as the native complex, 1-OH with Ser237 and Arg274, 3-OH with Tyr143 and Ser278. While the electron density around the ligand is unambiguous, the broad cloud of electron density around Gln305 (loop 6–7) (Fig. 2) can be interpreted as a statistical distribution of two conformers. In the crystal structure of VDR-1α,25(OH)$_2$D$_3$, the 25-OH group is hydrogen bonded to His305 and His397, His305 being the hydrogen bond acceptor and His397 the donor. Based on this information, we modeled Gln305 with its carbonyl oxygen as the hydrogen bond acceptor (Fig. 2). Structure refinement was done by using alternative conformations of Gln305.

The mutation from His305 to Gln305 changes the conformation of local region from Val300 in Helix 6 to Glu311 in Helix 7. This conformational change does not affect the ligand conforma-

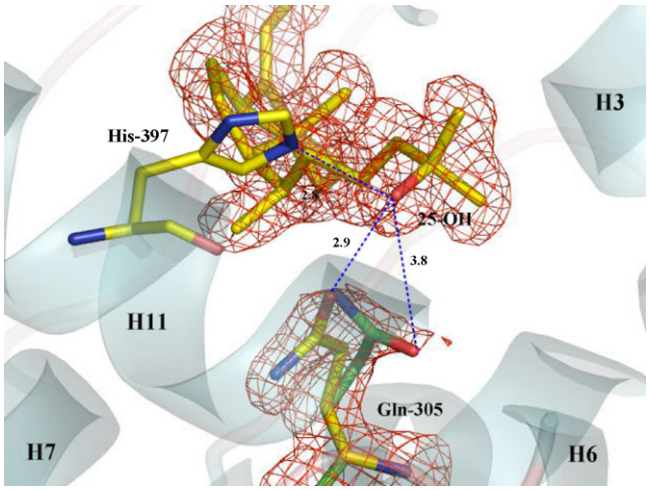

Fig. 2. The δ_A-weighted Fo–Fc omit map of VDR H305Q-1α,25(OH)$_2$D$_3$ complex is shown contoured at 3.0 δ (red). Conformation A (yellow) and conformation B (green) of Gln305 are shown. His397 and 1α,25(OH)$_2$D$_3$ are shown in yellow. Oxygen and nitrogen atoms are shown in red and blue, respectively. Hydrogen bonds are shown in blue dotted lines. Secondary structure of VDR is shown in cyan and H3, H6, H7, and H11 indicate helices. (For interpretation of the references to color in this figure legend, the reader is referred to the web version of the article.)

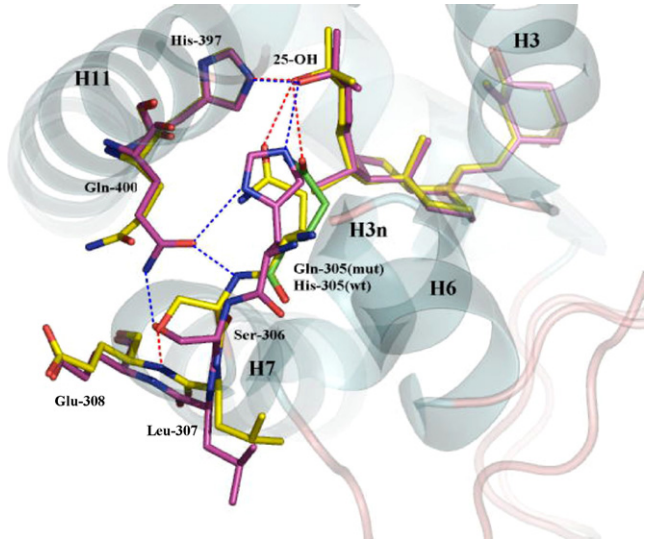

Fig. 3. Close-up view around Gln305 mutation site. The wt VDR-1α,25(OH)$_2$D$_3$ complex (magenta) and VDR H305Q-1α,25(OH)$_2$D$_3$ complex (yellow and green) are shown, after superimposed VDR complexes. Two conformations of Gln305 are shown in yellow and green, respectively. Oxygen and nitrogen atoms are shown in red and blue, respectively. Hydrogen bonds of wt VDR and VDR H305Q are shown in blue and red dotted lines, respectively. Secondary structure of VDR is shown in cyan and H3n, H3, H6, H7, and H11 indicate helices. (For interpretation of the references to color in this figure legend, the reader is referred to the web version of the article.)

tion. In the wild-type VDR-1α,25(OH)$_2$D$_3$ structure, an hydrogen bond network is observed between the 25-OH of the ligand, His305, Gln400, and Ser306 (Fig. 3). In the present crystal structure, the hydroxyl group of Ser306 points towards a different direction and the hydrogen bond between Ser306 with Gln400 is lost. As a result, the conformation of Gln400 becomes flexible, the hydrogen bond of Gln400 with Gln305 disappears, and Gln305 adopts alternative conformation (A- and B-form). These observations are consistent with the broad and weak electron density for Gln305 and Gln400, respectively. The hydrogen bond of the 25-OH group with His397 (2.8 Å) is similar to that of wt VDR-1α,25(OH)$_2$D$_3$ structure (2.8 Å). On the other hand, the distance of 25-OH with Gln305 is 2.9 Å for the A conformer and 3.8 Å for the B conformer (Fig. 2). The later is indicative of a weaker hydrogen bond. Altogether the H305Q mutation induces a conformational change that results in the loss of two H-bonds (Ser306–Gln400 and Gln400–His305) which in turn loosen Gln305 that adopts two different conformations. Our results are in agreement with an observed 8-fold lower binding affinity for 1α,25(OH)$_2$D$_3$ to VDR H305Q mutant [11].

In conclusion, the VDR H305Q-1α,25(OH)$_2$D$_3$ complex structure shows almost same conformation as the wild-type VDR-1α,25(OH)$_2$D$_3$ complex. Only local conformational change around Gln305 affects the stability of VDR H305Q and the binding to 1α,25(OH)$_2$D$_3$. The high-resolution structure of disease-associated protein provides the structural basis for a rational approach to the design of more potent ligands that can compensate for the H305Q mutation.

Protein data bank accession number

The accession number for the coordinates of the structures VDR H305Q/1α,25(OH)$_2$D$_3$ reported in this article is 3M7R.

Acknowledgments

We thank the staff of the beamline BM30 at the European Synchrotron Radiation Facility (ESRF, Grenoble, France) for excellent technical assistance. The study described here was supported by CNRS, INSERM, ULP, the European Commission as SPINE2-complexes (LSHG-CT-2006-031220) under the RDT programme 'Quality of Life and Management of Living Resources'.

References

[1] H.F. DeLuca, Overview of general physiologic features and functions of vitamin D, Am. J. Clin. Nutr. 80 (6 Suppl.) (2004) 1689S–1696S.
[2] G.N. Hendy, K.A. Hruska, S. Mathew, D. Goltzman, New insights into mineral and skeletal regulation by active forms of vitamin D, Kidney Int. 69 (2006) 218–223.
[3] S. Christakos, P. Dhawan, P. Benn, A. Porta, M. Hediger, G.T. Oh, E.B. Jeung, Y. Zhong, D. Ajibade, K. Dhawan, J. Joshi, Vitamin D: molecular mechanism of action, Ann. N. Y. Acad. Sci. 1116 (2007) 340–348.
[4] R. Bouillon, G. Carmeliet, L. Verlinden, E. van Etten, A. Verstuyf, H.F. Luderer, L. Lieben, C. Mathieu, M. Demay, Vitamin D and human health: lessons from vitamin D receptor null mice, J. Steroid Biochem. Mol. Biol. 29 (2008) 726–776.
[5] R. Koren, Vitamin D receptor defects: the story of hereditary resistance to vitamin D, Pediatr. Endocrinol. Rev. 3 (Suppl. 3) (2007) 470–475.
[6] U.A. Liberman, Vitamin D-resistant diseases, J. Bone Miner. Res. 22 (Suppl. 2) (2007) V105–V107.
[7] P.J. Malloy, R. Xu, A. Cattani, L. Reyes, D. Feldman, A unique insertion/substitution in helix H1 of the vitamin D receptor ligand binding domain in a patient with hereditary 1,25-dihydroxyvitamin D-resistant rickets, J. Bone Miner. Res. 19 (2004) 1018–1024.
[8] K. Kristjansson, A.R. Rut, M. Hewison, J.L. O'Riordan, M.R. Hughes, Two mutations in the hormone binding domain of the vitamin D receptor cause tissue resistance to 1,25 dihydroxyvitamin D3, J. Clin. Invest. 92 (1993) 12–16.
[9] G.K. Whitfield, S.H. Selznick, C.A. Haussler, J.C. Hsieh, M.A. Galligan, P.W. Jurutka, P.D. Thompson, S.M. Lee, J.E. Zerwekh, M.R. Haussler, Vitamin D receptors from patients with resistance to 1,25-dihydroxyvitamin D3: point mutations confer reduced transactivation in response to ligand and impaired interaction with the retinoid X receptor heterodimeric partner, Mol. Endocrinol. 10 (1996) 1617–1631.
[10] M.R. Haussler, C.A. Haussler, P.W. Jurutka, P.D. Thompson, J.C. Hsieh, L.S. Remus, S.H. Selznick, G.K. Whitfield, The vitamin D hormone and its nuclear receptor: molecular actions and disease states, J. Endocrinol. (September (154 Suppl.)) (1997) S57–S73.
[11] P.J. Malloy, T.R. Eccleshall, C. Gross, L. Van Maldergem, R. Bouillon, D. Feldman, Hereditary vitamin D resistant rickets caused by a novel mutation in the vitamin D receptor that results in decreased affinity for hormone and cellular hyporesponsiveness, J. Clin. Invest. 99 (1997) 297–304.
[12] P.J. Malloy, W. Zhu, X.Y. Zhao, G.B. Pehling, D. Feldman, A novel inborn error in the ligand-binding domain of the vitamin D receptor causes hereditary vitamin D-resistant rickets, Mol. Genet. Metab. 73 (2001) 138–148.
[13] P.J. Malloy, R. Xu, L. Peng, P.A. Clark, D. Feldman, A novel mutation in helix 12 of the vitamin D receptor impairs coactivator interaction and causes hereditary 1,25-dihydroxyvitamin D-resistant rickets without alopecia, Mol. Endocrinol. 16 (2002) 2538–4256.

[14] P.J. Malloy, R. Xu, L. Peng, S. Peleg, A. Al-Ashwal, D. Feldman, Hereditary 1,25-dihydroxyvitamin D resistant rickets due to a mutation causing multiple defects in vitamin D receptor function, Endocrinology 145 (2004) 5106–5114.
[15] N. Rochel, J.M. Wurtz, A. Mitschler, B. Klaholz, D. Moras, The crystal structure of the nuclear receptor for vitamin D bound to its natural ligand, Mol. Cell 5 (2000) 173–179.
[16] N. Rochel, D. Moras, Ligand binding domain of vitamin D receptors, Curr. Top. Med. Chem. 6 (2006) 1229–1241.
[17] P. Antony, R. Sigüeiro, T. Huet, Y. Sato, N. Ramalanjaona, L.C. Rodrigues, A. Mouriño, D. Moras, N. Rochel, Structure–function relationships and crystal structures of the vitamin D receptor bound 2 alpha-methyl-(20S,23S)- and 2 alpha-methyl-(20S,23R)-epoxymethano-1 alpha,25-dihydroxyvitamin D3, J. Med. Chem. 53 (2010) 1159–1171.
[18] Z. Otwinowski, W. Minor, Processing of X-ray data collected in oscillation mode, Methods Enzymol. 276 (1997) 307–326.
[19] A.T. Brunger, P.D. Adams, G.M. Clore, W.L. DeLano, P. Gros, R.W. Grosse-Kunstleve, J.S. Jiang, J. Kuszewski, M. Nilges, N.S. Pannu, et al., Crystallography & NMR system: a new software suite for macromolecular structure determination, Acta Crystallogr. D: Biol. Crystallogr. 54 (1998) 905–921.
[20] T.A. Jones, J.Y. Zou, S.W. Cowan, Kjeldgaard, Improved methods for building protein models in electron density maps and the location of errors in these models, Acta Crystallogr. A 47 (1991) 110–119.
[21] N. Rochel, G. Tocchini-Valentini, P.F. Egea, K. Juntunen, J.M. Garnier, P. Vihko, D. Moras, Functional and structural characterization of the insertion region in the ligand binding domain of the vitamin D nuclear receptor, Eur. J. Biochem. 268 (2001) 971–979.